Progress In Electromagnetics Research C, Vol. 86, 29–39, 2018

Wideband High-Efficiency Fresnel Zone Plate Reflector Antennas Using Compact Subwavelength Dual-Dipole Unit Cells

Xin Liu, Yin-Yan Chen, and Yuehe Ge*

Abstract—In this paper, wideband high-efficiency Fresnel zone plate (FZP) reflector antennas are investigated and developed. Two simple dual-dipole unit cells with different periodicity sizes are first characterized for the design of Fresnel zone plate reflector antennas. The gain bandwidth of the FZP reflector antennas is then theoretically investigated using the two unit cells. Based on the results, a wideband high-efficiency FZP reflector containing 15 correcting zones is designed using the unit cell with a smaller size and quarter-wavelength correction phases. A standard pyramidal horn and a slot-fed patch antenna are applied to feed the FZP reflector alternately. With a feed horn, the wideband high-efficiency radiation performance including a peak gain of 32.1 dBi and an aperture efficiency of 58.2% can be achieved. By using the designed planar feeder, a compact FZP reflector antenna can be obtained with compromised radiation performance. All are demonstrated by experiments.

1. INTRODUCTION

Printed reflectarray antennas [1–10] have been rapidly developed in the recent decade due to their advantages over their parabolic counterparts, including lower mass and volume, low profile, ease of manufacture, and possibilities of beam shaping and electronic beam controlling. Reflectarray antennas combine the benefits of parabolic reflectors and phased-arrays, and their applications can be found in millimeter-wave radar, communication and automotive cruise systems [11]. Generally, there are two types of reflectarrays: one is based on the continuous phase-correcting technique [2–7], and the other is designed using the Fresnel zone principle [8–10]. Reflectarrays with continuous phase compensation have relatively high radiation efficiency but need a phase correction range of 360°, which would affect the element size and thickness. Fresnel zone plate (FZP) reflector antennas [8–10, 12–14], however, have lower efficiency and hence gained fewer applications in the past. Recently, artificial materials and metasurfaces have attracted more and more attention due to their capability to manipulate the amplitude and phase of incoming waves. Thin phase-correcting lenses [15, 16], which are low-profile, planar, and light-weight, are developed to exhibit a higher efficiency and can be applied to applications at microwave and millimeter-wave bands. Generally, planar FZP reflector antennas have the advantages of simple design principle, ease of fabrication and mounting, and hence low cost in some applications.

On the other hand, almost all the reflectarray antennas in the literature are fed by horn antennas [1–16], leading to bulky volumes. To make the reflectarray antennas and the corresponding systems compact and flat, planar feeding sources [17] or arrays are required.

The bandwidth of the reflectarray antenna can be normally improved by using multilayer designs [3, 4] or multiresonant elements [5–7]. Another effective method is to use compact subwavelength elements, as demonstrated in [18, 19]. One of the challenges using subwavelength elements in reflectarray antennas is fabrication tolerance, especially for those operating at millimeter-wave bands. To the

Received 2 May 2018, Accepted 23 July 2018, Scheduled 28 July 2018

* Corresponding author: Yuehe Ge (yuehe@ieee.org).

The authors are with the College of Information Science and Engineering, Huaqiao University, Xiamen, Fujian Province 361021, China.

authors' best knowledge, the compact subwavelength elements have not been studied in FZP reflector antennas. In this paper, single-layered dual-dipole unit cells with different subwavelength sizes are applied to study the bandwidth improvement of FZP reflector antennas. Numerical simulations are carried out to exhibit the bandwidth enhancement by employing the compact subwavelength unit cell. Based on the study, an offset-fed FZP reflector antenna with a single-layered dual-dipole unit cell of $\lambda/8 \times \lambda/4$ is developed and fabricated. The measurements demonstrate that both broad gain-bandwidth and high efficiency, which is comparable to normal high-efficiency reflectarray antennas, are achieved. In addition, a planar feeder is developed, and a center-fed FZP reflector antenna is constructed and tested.

2. UNIT CELL DESIGNS FOR FZP REFLECTORS

A single-layered dual-dipole unit cell has been proposed [20–22] to investigate the reflectarray antenna with continuous phase compensation. As shown in Fig. 1, the concerned unit cells consist of one dielectric layer, two metallic dipoles, and a conducting ground. The two metallic dipoles, which have different sizes, are printed on the two sides of the dielectric layer. An air gap, with a height of h, is inserted between the dielectric layer and the ground. By controlling the lengths (L_b and L_t) of the two dipoles of each unit cell periodically forming the FZPs, the required compensation phases can be obtained. The characterization of the unit cells and the simulations of the FZPs below were carried out using the commercial software Ansys HFSS.

In order to investigate the gain bandwidths of the concerned FZPs, two unit cells with different sizes are applied. Figs. 1(a) and 1(b) depict the two unit cells, respectively, which have similar configuration and size in x direction but different sizes in y direction. In practical designs, the surface sizes of the two unit cells are $\lambda/4 \times \lambda/4$ and $\lambda/8 \times \lambda/4$, respectively. In this work, the design frequency is 24 GHz. An Arlon AD255 substrate, which has the dielectric constant of 2.55 and thickness of 0.5 mm (t), is used to construct the FZPs. The other parameters are: $d = 3.125$ mm (0.25λ) and $h = 1$ mm. To achieve a stable and smooth reflection phase range, the dipole length on the lower side of the substrate, L_b, was set to be a constant, while that on the upper side, L_t, was varied. It was expected that the required

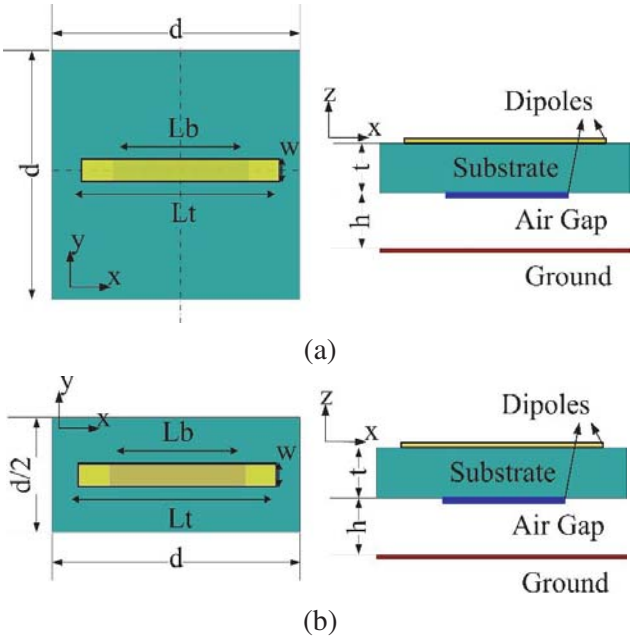

Figure 1. Basic unit cells for FZPs: (a) cell 1 with a size of $\lambda/4 \times \lambda/4$; (b) cell 2 with a size of $\lambda/8 \times \lambda/4$.

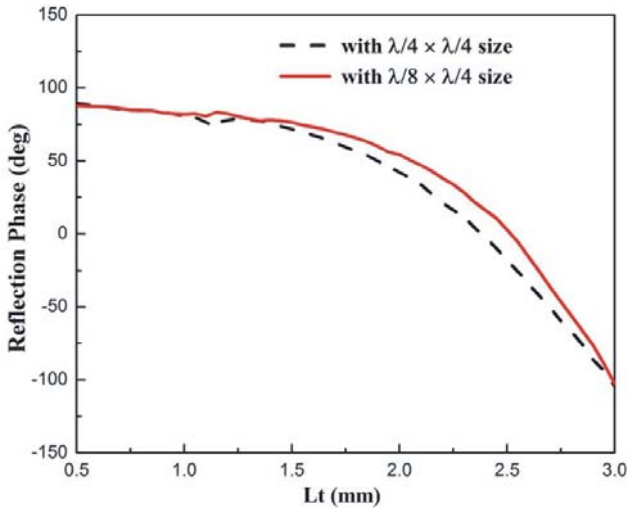

Figure 2. Reflection phases versus L_t at 24 GHz.

compensation phases when forming the FZPs would be obtained by changing the parameter L_t. The simulated results for the two different unit cells are plotted in Fig. 2. It can be seen that the reflection phase ranges for both cells are similar and over 180°. The different sizes of the two unit cells will not result in an outstanding phase difference. However, by using the results, the reflection phases −90°, 0°, and 90° can be achieved to perform the phase correction when constructing FZP reflectors.

3. FZP REFLECTORS AND SIMULATION RESULTS

3.1. Design Principle of FZP Reflectors

When designing Fresnel zone plate reflectors, the reflectors are divided into zones where constant phases are applied to compensation, as shown in Figs. 3(a) and (b), which depict a center-fed and an offset-fed Fresnel zone plate reflectors, respectively. The compensation phases φ_i for the center-fed one are determined by the phase correction step, integer P, while the phase correction order and the radii of Fresnel zones are related using classical formulas

$$r_i = \sqrt{2if\frac{\lambda}{P} + \left(i\frac{\lambda}{P}\right)^2} \tag{1}$$

$$\varphi_i = \frac{(i-1)\,k\lambda}{P} \tag{2}$$

where f is the focal length, i the order of the Fresnel zone, λ the free space wavelength at the center frequency, and P the number of phase correction. The Fresnel zones include a centered circular zone and many concentric circular ring zones, whose widths are determined by $(r_i - r_{i-1})$ and will decrease with the increase of the order i. Different from the focusing antennas designed using the phase-correction techniques, which requires a large number of basic elements to provide almost continuous phase compensation from 0° to 360°, the number of elements the FZP reflectors needed is equal to P. The bandwidth and efficiency performances of the FZP reflectors are improved when the number P increases [7–10]. However, due to the limitation of element sizes, most FZP antennas, including reflectors and lens, need more complicated elements to accommodate the Fresnel zones to perform the phase correction when the number P increases [2], resulting in difficulty in fabrications, especially at millimeter-wave bands.

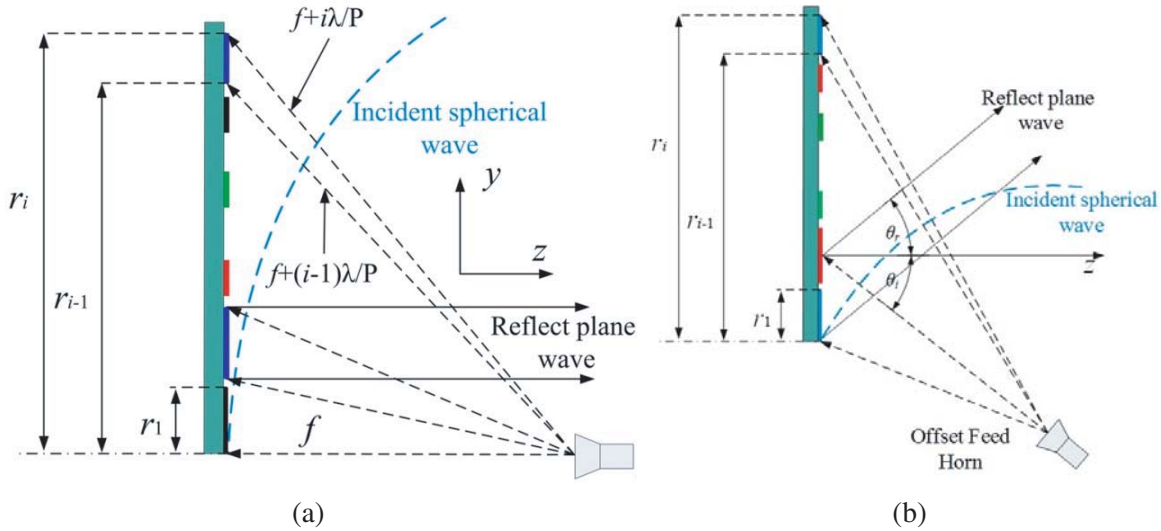

Figure 3. Definition of the Fresnel zones: (a) center-fed case; (b) offset-fed case.

3.2. FZP Reflector Designs and Simulated Results

In the characterizations of the two concerned unit cells in Section 2, over 180° reflection phase ranges are obtained. Three reflection phases, −90°, 0°, and 90°, are able to be applied to the phase correction. Therefore, quarter-wavelength FZP reflectors ($P = 4$) can be designed using the two unit cells. The rest correction phase of 180° in the quarter-wavelength FZP reflectors can be easily obtained by using metallic patch. Fig. 4 shows two elements that are composed of a thick metallic patch and four unit cells shown in Section 2. They have the same dimensions but differently polarized incident waves. As shown in Figs. 4(a) and 4(b), the polarizations of the incident waves are parallel and perpendicular to the metallic patches respectively. Simulated results show that the reflection phases for the two cases are about 183° and 175°, respectively. Therefore, the metallic patches shown in Fig. 4 can be applied in the Fresnel zones that need to provide the reflection phase of 180°.

Based on the two unit cells and metallic patches, two 10-zone Fresnel reflectors, operating at 24 GHz, have been eventually designed. The two designs have the same diameter, 140 mm. A standard

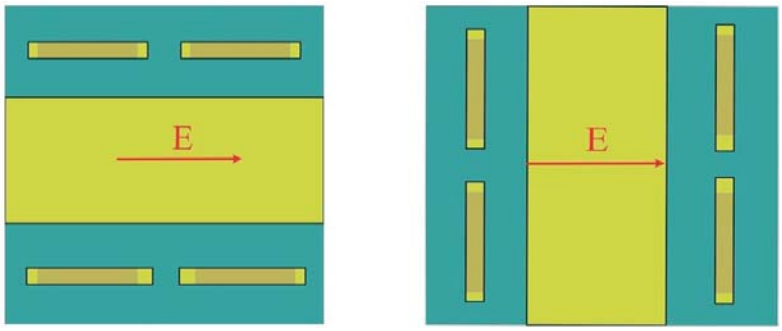

(a) (b)

Figure 4. The unit cells with the reflection phase of 180° for differently polarized incident waves: (a) horizontal polarization; (b) vertical polarization.

Table 1. Crucial parameters of the two unit cells for the two FZP reflector designs.

	Refl. phases	90°	0°	−90°
Cell 1	L_t (mm)	0.5	2.52	2.95
Cell 2	L_t (mm)	0.5	2.37	2.93

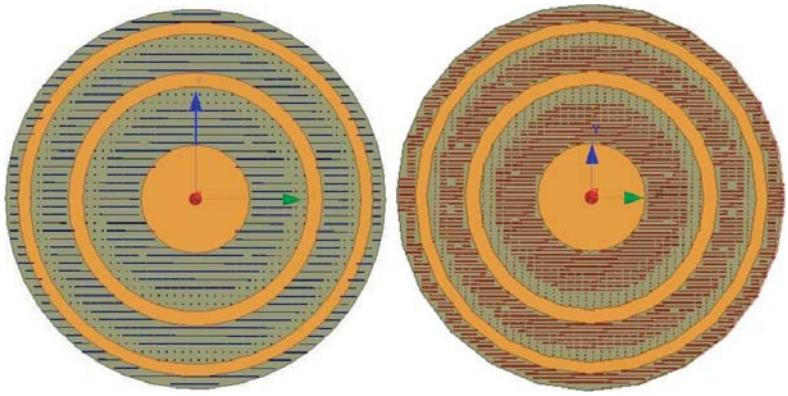

(a) (b)

Figure 5. FZP reflectors with the unit cell size of: (a) $\lambda/4 \times \lambda/4$, and (b) $\lambda/8 \times \lambda/4$.

pyramidal horn, which has a gain of 15 dBi at 24 GHz, is used as the feeder for both antennas. The focal lengths are also the same, 70 mm. Therefore, the f/D value is 0.5. Cell 1 and cell 2, which have the sizes of $\lambda/4 \times \lambda/4$ and $\lambda/8 \times \lambda/4$, respectively, are applied to construct Antenna I and Antenna II, respectively. The crucial parameters of the two unit cells with different reflection phases are listed in Table 1. Other common parameters include $L_b = 0.5$ mm, $w = 0.25$ mm, $d = 3.125$ mm, $t = 0.5$ mm, and $h = 1$ mm. Figs. 5(a) and 5(b) show the surface views of the two reflectors, respectively.

The two antenna designs were simulated by the commercial software Ansys HFSS. The simulated gains are plotted in Fig. 6. It can be seen that both antennas have similar peak gains, about 26.5 dBi, while the gain bandwidth of Antenna II is apparently better. The 1-dB and 3-dB gain bandwidths are 8.0% and 24% for Antenna I and 19.2% and 33% for Antenna II. The simulated radiation patterns are shown in Fig. 7. It can be seen that both antennas have very low cross-polarization levels. Antenna II has lower sidelobe levels than Antenna I in both E and H planes. With a compact unit cell, Antenna II exhibits better gain bandwidths and sidelobe levels, without compromising other radiation performances.

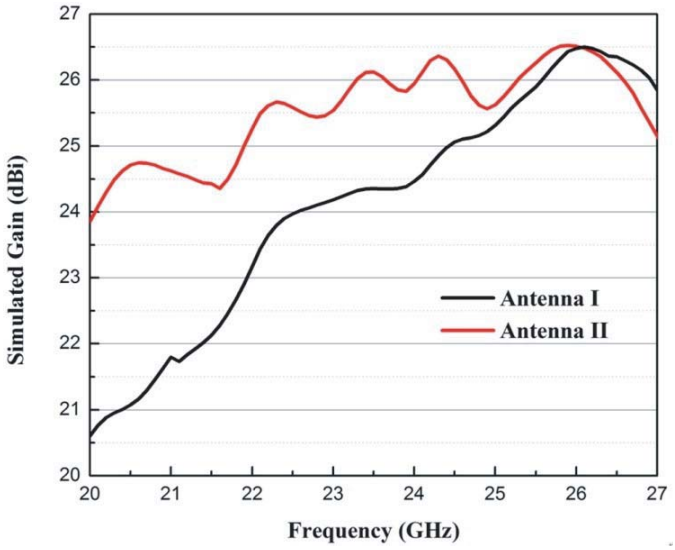

Figure 6. Simulated gain curves of the two FZP antenna designs.

4. PROTOTYPE AND MEASUREMENT RESULTS

4.1. FZP Reflector Fabrication

After the theoretical demonstration of the radiation performance of the FZP antennas based on the two unit cells of different sizes, an FZP reflector prototype formed by cell 2 was fabricated. The prototype has 15 Fresnel zones totally, and the diameter is 210 mm. The designed metallic arrays are printed on an Arlon AD255 substrate, which has a dielectric constant of 2.55 and thickness of 0.5 mm, as shown in the inset of Fig. 8. The total thickness of the FZP reflector is 1.5 mm or 0.125λ (where λ is the free-space wavelength at 24 GHz). The primary source feeding the FZP reflector will be placed 105 mm away from the reflector. The value of f/D is 0.5. It is well known that the influence of the feed blockage will seriously affect the measurement results. On the other hand, almost all the feeding sources of reflector antennas in literatures are horn antennas or open-end waveguides [1–16], leading to bulky volumes. To make the reflector antennas compact, it is necessary to investigate the application of planar feeding sources to reflector antennas. In this section, two different feeders, a standard pyramidal horn and a planar slot-fed patch antenna, are alternately applied to feed the FZP reflector. Measurements are carried out for FZP reflector antennas with both feeders.

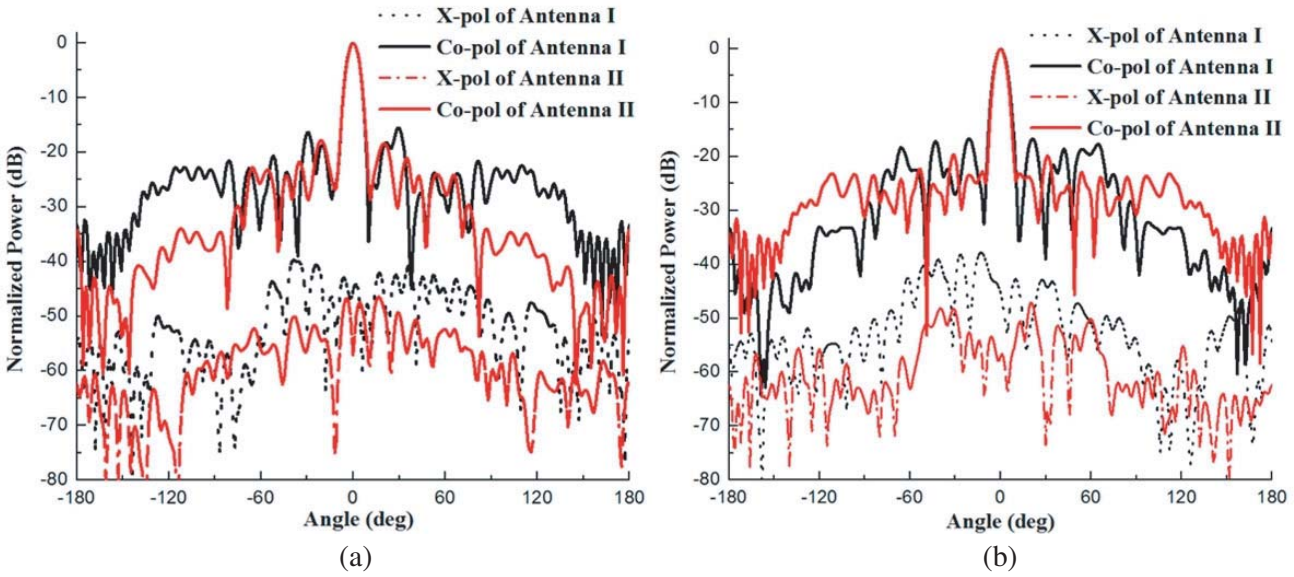

Figure 7. Simulated radiation patterns at 24 GHz for the two antennas in: (a) E-plane, (b) H-plane.

4.2. Offset Horn Feeder and the Measured Results

The measurement setup of the FZP reflector antenna prototype in an anechoic chamber is shown in Fig. 8. The far-field measurement system was applied to obtain the radiation performance. A standard linearly-polarized gain horn is first used to feed the FZP reflector. In order to investigate the effect of the feed blockage and the beam-steering performance, the horn is placed with offset angles of 0°, 10°, 20°, and 30°, alternately. During the placements with different offset angles, the aperture of the horn always points to the center of the FZP reflector. The tilted angles of directions of the reflected beams with different offset incident angles are theoretically 0°, 10°, 20°, and 30° with respect to the normal direction of the reflector, opposite to the feeding horn.

The measured radiation patterns are shown in Fig. 9. It can be seen that the directions of the main beams with different offset feeding angles conform to the prediction above. The radiation patterns with the offset feeding angle of 0°, as predicted, have been seriously affected by the feeder blockage. Reasonable radiation patterns are obtained when offset angles of the horn are 10°, 20°, and 30°, as shown in Fig. 9(a), though the gain reduction is observed with the increase of the offset feeding angle.

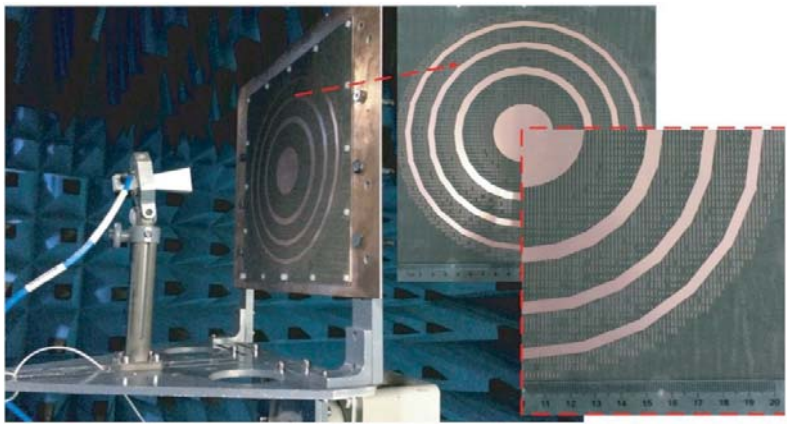

Figure 8. Fabricated prototype of the 15-zone FZP reflector antenna and the measurement setup in the anechoic chamber.

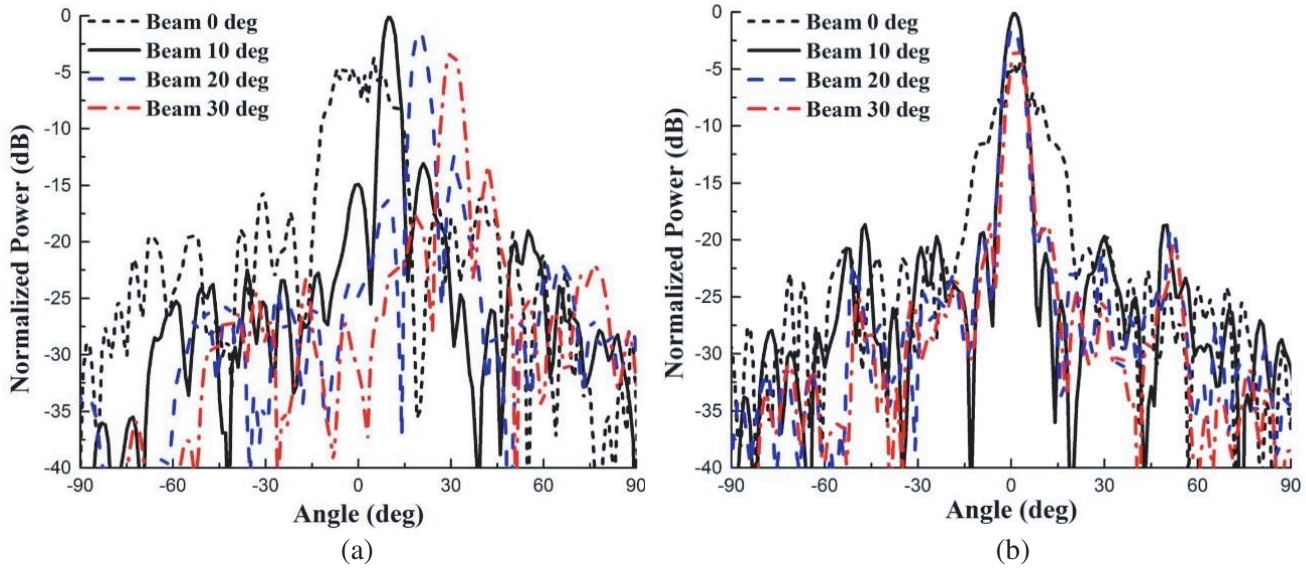

Figure 9. Measured radiation patterns with different offset feeding angles for the designed FZP reflector antenna at 24 GHz in: (a) E-plane, (b) H-plane.

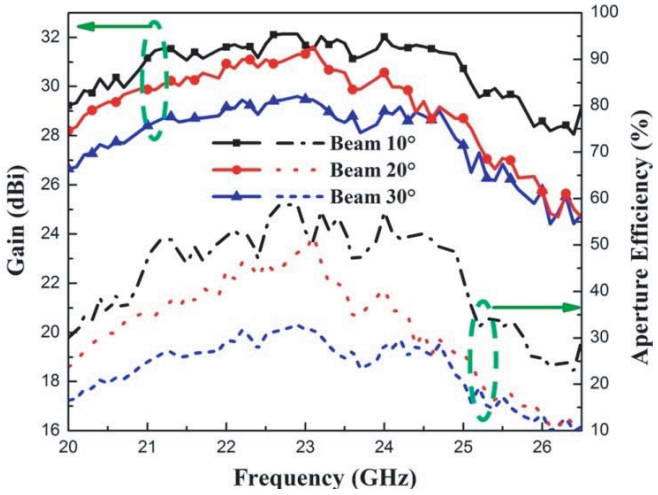

Figure 10. Measured gains and efficiencies for the different offset cases.

Compared to the result with the offset angle of 10°, which exhibits the best peak gain, the measured results show gain reductions of about 1.4 dB and 3 dB for the offset feeding angles of 20° and 30°, respectively. The effects of the feeder blockage for the center feeding case and the gain reduction for the different offset feeding cases can also be observed in the measured radiation patterns in the H plane shown in Fig. 9(b). It is also observed that the sidelobe level for the 10° beam case is about −14 dB in the E plane and −20 dB in the H plane. With the increase of the offset feeding angles, the sidelobe levels will deteriorate in the E plane. The patterns in the H plane exhibit better sidelobe levels, which will not change much with the change of the offset feeding angle. It can be seen that the reflectarray in Fig. 8 is designed to be a center geometry, which needs a symmetrical illumination to exhibit good radiation performance, as plotted in Figs. 6 and 7. The offset feed in Fig. 8 generates asymmetrical and symmetrical illuminations in the E and H planes, respectively, resulting in the different sidelobe levels in the two planes. The sidelobe levels in the E plane can be reduced using the reflectarray with an offset geometry.

The gains with the three offset feeding angles are measured and depicted in Fig. 10. The aperture efficiencies are estimated based on the measured results and also plotted in Fig. 10. The results with 10° offset angle give the best gain, 3-dB gain bandwidth and aperture efficiency, which are 32.1 dBi, 24.9%, and 58.2%. Table 2 summarizes the measured performance of the FZP reflector antenna.

Table 2. Summarization of the measured radiation performance of the FZP reflector antenna with a horn feeder.

Offset angle	SLLs (dB)		Peak gain	Gain BW	Aperture efficiency
10°	E-plane	−14	32.1 dBi	24.9% (3-dB) 17.4% (1-dB)	58.2%
	H-plane	−21			
20°	E-plane	−13	31.6 dBi	21.2% (3-dB)	52%
	H-plane	−20			
30°	E-plane	−11	29.6 dBi	24.1% (3-dB)	32.7%
	H-plane	−18			

4.3. Planar Antenna Feeder and the Measured Results

In order to obtain a compact FZP reflector antenna, a planar slot-fed patch antenna (SFPA) is designed to feed the FZP reflector. Fig. 11 shows the geometry of the slot-fed patch antenna, which consists of two substrates stacked with no air gap, a microstrip feedline on the bottom surface of the lower substrate, a ground with a rectangular slot on the top surface of the lower substrate, and a rectangular metallic patch on the top surface of the upper substrate. As shown in Fig. 11, the microstrip feedline will feed the rectangular patch through a rectangular slot on the ground. Both substrates use F4B, which has a dielectric constant of 2.55 and thicknesses of t_1 and t_2, respectively. The parameters of the antenna are shown in Fig. 11(a). The final dimensions of the SFPA are: $L_p = 34$ mm, $W_p = 16$ mm, $L_1 = 5$ mm, $W_1 = 3$ mm, $L_a = 4$ mm, $W_a = 0.3$ mm, $W_f = 1.8$ mm, $L_s = 1$ mm, $t_1 = 0.5$ mm, and $t_2 = 1.5$ mm. A prototype is fabricated and shown in Fig. 11(b). The planar feeder prototype is first measured, and the results are depicted in Fig. 12. The return loss larger than 10 dB is obtained from 20 GHz to 25 GHz, as shown in Fig. 12(a). The measured radiation pattern in the H plane is plotted in Fig. 12(b), together with that of the standard horn for comparison. It is apparent that the SFPA has a wider beamwidth. The measured peak gain is about 7 dBi.

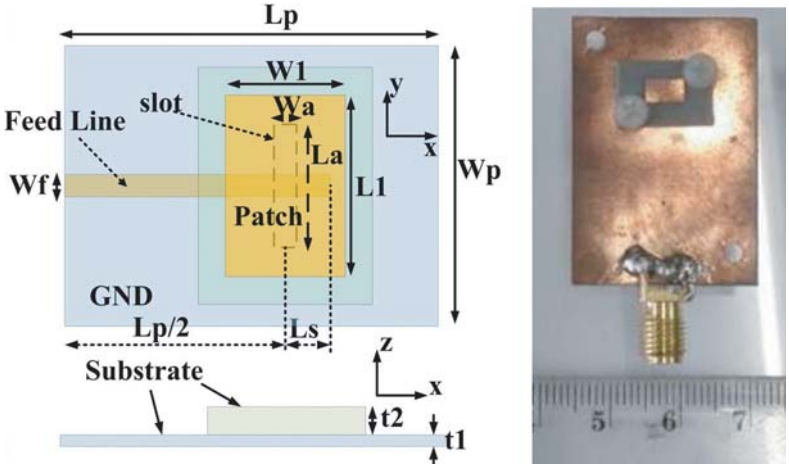

(a) (b)

Figure 11. The slot-fed patch antenna feeder: (a) geometry; (b) prototype.

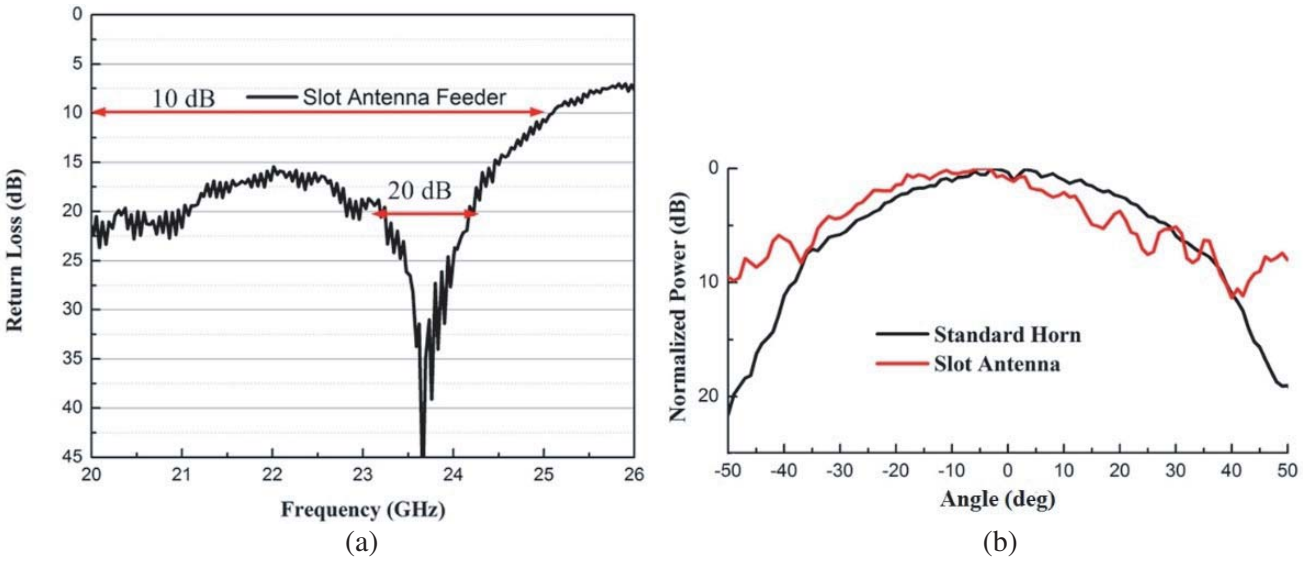

Figure 12. Measured return loss and radiation pattern of the slot-fed patch antenna: (a) return loss; (b) comparison of the radiation patterns between the feed horn and the slot-fed patch antenna.

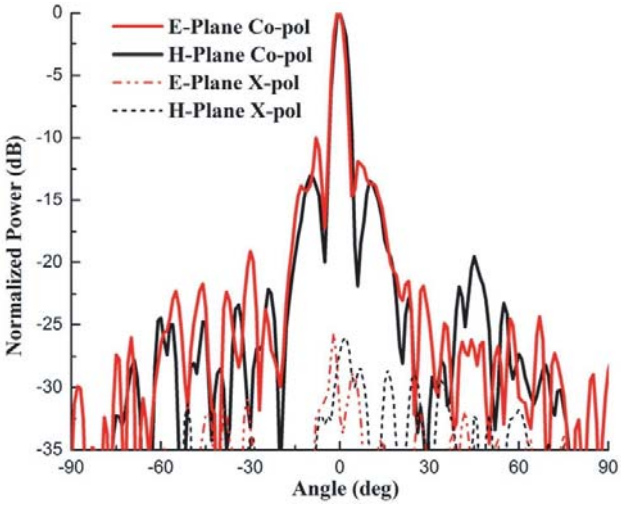

Figure 13. Measured radiation patterns of the FZP reflector antenna fed by the slot-fed patch antenna.

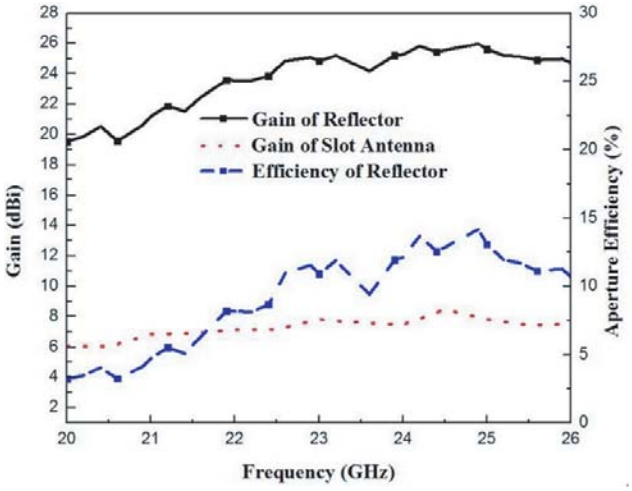

Figure 14. Measured gain and efficiency of the FZP reflector antenna fed by the slot-fed patch antenna.

The slot-fed patch antenna is then used to feed the above FZP reflector. In this case, the planar feeder is placed above the center of the FZP reflector, with a distance of 105 mm and no offset angle. The center-fed antenna was measured. The radiation patterns at 24 GHz are depicted in Fig. 13 and exhibit reasonable shapes. The effect of the feeder blockage cannot be observed in the patterns. However, the sidelobe levels, both in the E and H planes, are higher than those when using the feed horn. The gains of the FZP reflector antenna and the SFPA only are plotted in Fig. 14. With a peak gain of 26 dBi and 1-dB gain bandwidth of 14%, the peak efficiency, also shown in Fig. 14, is reduced to be 14.6%.

Due to the use of the SFPA, the gain and efficiency of the FZP reflector antenna are reduced. The SFPA has a wider beamwidth than the standard horn, outstanding different beamwidths in E and H planes, a different phase center, and asymmetrical radiation patterns in the E plane, which will deteriorate the radiation performance of the FZP reflector antenna, because the FZP reflector is

designed based on the phase center of a standard horn that has the symmetrical radiation patterns and the special −10 dB beamwidth. Among them, the phase errors caused by the different phase centers of feeders would seriously affect the performance of the antenna. With the fixed focusing length (105 mm) the wider beamwidth will cause extra spill-over loss and hence decrease the aperture efficiency.

To improve the aperture efficiency, a planar antenna with symmetrical radiation patterns is considered. A 2×2 antenna array, which has relatively symmetrical radiation patterns in both E and H planes, a −10-dB beamwidth of 85° in both E and H planes, and a gain of about 10.5 dBi at 24 GHz, is applied as the feeder of the reflectarray. Simulations from Ansys HFSS show that outstanding improvements on the aperture efficiency are obtained. With a focusing length of 115 mm, an aperture efficiency of more than 40% is achieved, which is close to those when using a horn as the feeder in Section 4.1.

5. CONCLUSION

Unit cells of different sizes exhibiting similar reflection phase ranges are applied to investigate the high-efficiency Fresnel zones plate reflector antennas. Theoretical simulations show that the FZP reflector antenna formed by the compact unit cell will provide a better gain bandwidth and higher gain and aperture efficiency. A high-efficiency FZP reflector antenna with different offset feeding angles is then designed, fabricated, and tested. The measured results show that a peak gain of 32.1 dBi, an efficiency of 58.2% and a 3-dB gain bandwidth of 24.9% are achieved with a standard feed horn. A planar slot-fed patch antenna is also developed to feed the FZP reflector to make the antenna compact and flat. The measurement results achieve a peak gain of 26 dBi and an efficiency of 14.6%. Further development of planar feeder will be carried out to achieve compact high-efficiency FZP reflector antennas, especially operating at millimeter-wave bands.

ACKNOWLEDGMENT

This research was supported by the Foreign Cooperation Projects in Fujian Province (2016I0008), China, the Foreign Cooperation Projects of Quanzhou Science and Technology Bureau (2017T005), China, and the Subsidized Projects for Cultivating Postgraduates' Innovative Ability in Scientific Research of Huaqiao University (1611301025).

REFERENCES

1. Huang, J. and J. A. Encinar, *Refectarray Antennas*, John Wiley & Sons, Institute of Electrical and Electronics Engineers, 2008.
2. Hasani, H., M. Kamyab, and A. Mirkamali, "Broadband reflectarray antenna incorporating disk elements with attached phase-delay lines," *IEEE Antennas Wireless Propag. Lett.*, Vol. 9, 156–158, 2010.
3. Encinar, J. A. and J. A. Zomaza, "Broadband design of three-layer printed refectarrays," *IEEE Trans. Antennas Propag.*, Vol. 51, No. 7, 1662–1664, Jul. 2003.
4. Chang, T. N. and H. Suchen, "Microstrip reflectarray with QUAD-EMC element," *IEEE Trans. Antennas Propag.*, Vol. 53, No. 5, 1993–1997, Jun. 2005.
5. Chaharmir, M. R., J. Shaker, M. Cuhaci, and A. Ittipiboon, "A broadband reflectarray antenna with double square rings," *Microwave and Optical Technology Letters*, Vol. 48, No. 7, 1317–1320, Jul. 2006.
6. Li, Q. Y., Y. C. Jiao, and G. Zhao, "A novel microstrip rectangular patch/ring combination reflectarray element and its application," *IEEE Antennas Wireless Propag. Lett.*, Vol. 8, 1119–1122, 2009.
7. Guo, L., P.-K. Tan, and T.-H. Chio, "Bandwidth improvement of reflectarrays using single-layered double concentric circular ring elements," *Progress In Electromagnetics Research C*, Vol. 46, 91–99, 2014.

8. Nguyen, B. D., C. Migliaccio, Ch. Pichot, K. Yamamoto, and N. Yonemoto, "W-band Fresnel zone plate reflector for helicopter collision avoidance radar," *IEEE Trans. Antennas Propag.*, Vol. 55, No. 5, 1452–1456, May 2007.
9. Nguyen, B. D., J. Lanteri, J. Dauvignac, C. Pichot, and C. Migliaccio, "94 GHz Folded Fresnel reflector using C-patch elements," *IEEE Trans. Antennas Propag.*, Vol. 56, 3373–3381, 2008.
10. Tayebi, A., J. Gomez, I. Gonzalez, and F. Catedra, "Influence of the feed location on the performance of a conformed Fresnel zone reflector," *IEEE Antennas Wireless Propag. Lett.*, Vol. 12, 547–550, 2013.
11. Huder, B. and W. Menzel, "Flat printed reflector antenna for mm-wave applications," *Electron. Lett.*, Vol. 24, No. 6, 318–319, Mar. 1988.
12. Hristov, H. D. and M. H. A. Herben, "Millimeter-wave Fresnel zone plate lens and antenna," *IEEE Trans. Microw. Theory Tech.*, Vol. 43, 2779–2785, Dec. 1995.
13. Guo, Y. J., I. H. Sassi, and S. K. Barton, "Multilayer offset Fresnel zone plate reflector," *IEEE Microwave and Guided Wave Letters*, Vol. 4, No. 6, Jun. 1994.
14. Guo, Y. J. and S. K. Barton, "Phase correcting zonal reflector incorporating rings," *IEEE Trans. Antennas Propag.*, Vol. 43, 350–354, Apr. 1995.
15. Chen, Y. and L. Chen, "A C-band flat lens antenna with double-ring slot elements," *IEEE Antennas Wireless Propag. Lett.*, Vol. 12, 341–344, 2013.
16. Gagnon, N., A. Petosa, and D. A. McNamara, "Printed hybrid lens antenna," *IEEE Trans. Antennas Propag.*, Vol. 60, No. 5, 2514–2518, May 2012.
17. Chen, L.-W. and Y. Ge, "A K-band flat transmitarray antenna with a planar microstrip slot-fed patch antenna feeder," *Progress In Electromagnetics Research C*, Vol. 64, 97–104, 2016.
18. Nayeri, P., F. Yang, and A. Z. Elsherbeni, "Bandwidth improvement of refectarray antennas using closely spaced elements," *Progress In Electromagnetics Research C*, Vol. 18, 19–29, 2011.
19. Nayeri, P., F. Yang, and A. Z. Elsherbeni, "Broadband refectarray antennas using double-layer sub-wavelength patch elements," *IEEE Antennas Wireless Propag. Lett.*, Vol. 9, 1139–1142, 2010.
20. Zeng, X. and Y. Ge, "Design of broadband polarization-sensitive reflectarray using a single-layer substrate and double printed dipole arrays," *Proc. 2014 Asia-Pacific Microwave Conf.*, Soeul, South Korea, Nov. 4–7, 2014.
21. Chen, Y. Y., Y. Ge, and T. S. Bird, "An offset reflectarray antenna for multipolarization applications," *IEEE Antennas Wireless Propag. Lett.*, Vol. 15, 1353–1356, 2016.
22. Ge, Y., Y. Y. Chen, Y. Liu, and L. Chen, "Designs of flat reflectarray and transmitarray antennas using the Fresnel zone principle," *Proc. 2016 IEEE 5th Asia-Pacific Conference on Antennas and Propagation (APCAP)*, 351–352, Kaoshiung, Taiwan, Jul. 26–29, 2016.